INTERNATIONAL JOURNAL OF RESEARCH IN MEDICAL SCIENCES & TECHNOLOGY

e-ISSN:2455-5134; p-ISSN: 2455-9059

A Comprehensive Analysis Of The Techniques In Unsupervised Machine Learning For Removing Artefacts In Electrodermal Activity

Krishna Rathi

Anil Surendra Modi School of Commerce, Narsee Monjee Institute of Management Studies, Mumbai

Paper Received: 28 October 2022; **Paper Accepted:** 21 November 2022; **Paper Published:** 24 December 2022

DOI: http://doi.org/10.37648/ijrmst.v14i01.022

How to cite the article:

Krishna Rathi, A Comprehensive Analysis Of The Techniques In Unsupervised Machine Learning For Removing Artefacts In Electrodermal Activity, IJRMST, July-December 2022, Vol 14, 199-208, DOI: http://doi.org/10.37648/ijrmst.v14i01.022

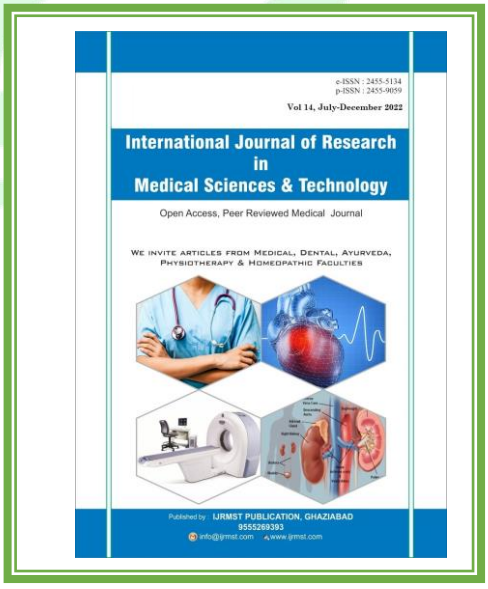

ABSTRACT

In any data preprocessing pipeline for physiological time series data, artefact detection and removal is an essential step, particularly when the data are obtained outside of controlled experimental circumstances. Given that these artefacts are frequently easily recognised with the naked eye, unsupervised machine learning methods seem like a viable alternative to manually labelled training datasets. Current techniques are frequently heuristic-based, non-generalizable, or designed for less artifact-prone, controlled experimental environments. In this work, we evaluate three such unsupervised learning techniques: K-nearest neighbour distance, isolation forests, and 1-class support vector machines. These algorithms are used to analyse electrodermal activity (EDA) data obtained during surgery in order to identify heavy cautery-related artefact. In order to provide inputs for the unsupervised learning techniques, we first defined 12 characteristics for every half-second frame. We contrasted the top-performing unsupervised learning technique for each subject with four other current approaches for the elimination of EDA artefacts. The only learning strategy that was successful in completely eliminating the artefact for each of the six subjects was unsupervised learning. In complex circumstances, this technique can be readily extended to different modalities of physiological data.

INTRODUCTION

The data are more prone to unforeseen and unpredictable sources of artefact and interference as it becomes more usual to collect physiological time series data outside of controlled laboratory settings in increasingly complicated naturalistic contexts. Most of these artefacts are easily visible to the unaided eye with little practice. Nevertheless, efforts to mechanise observables, like thresholding signal value or signal derivative, are not consistent between datasets and patients. In several other contexts, supervised learning—in which machine learning models use labelled training datasets to learn how to distinguish between signal and artifact—has proven to be extremely effective [1]. In the case of artefact detection, however, supervised learning is labour expensive and unfeasible since a large number of training datasets require the manual labelling of each short time increment of data. However, the majority of physiological time series data have clearly visible artefacts, indicating that artifactual data differ significantly from genuine signals. Since labelled training

sets are not necessary, unsupervised machine learning techniques provide an alternative that meets time and human labour restrictions while enabling the learning of more complicated patterns that are not explicitly documented [2].

In this study, we use only 12 well-defined characteristics to show the effectiveness of unsupervised learning algorithms for artefact detection in electrodermal activity (EDA) datasets [3]. Six human participants had lower abdominal surgery, and these data were continually gathered during the procedure. As a result, they were particularly vulnerable to motion and surgical cautery-related artefacts, which resulted in significant and obvious deflections in the data. To make matters more complicated, there are times when the EDA remains intact but displaced in between the huge deflections, even if these artifactual deflections are readily apparent. Furthermore, it is unclear where each deflection starts and ends. Lastly, different people and datasets have different deflections in terms of their amplitude, sharpness, and direction. An example dataset with labelled artefact attributes is shown in Figure 1.

The techniques currently available for removing artefacts from EDA are constrained and unique to the datasets they were tested on [4–8]. Typically, these datasets were gathered in experimental environments that were either completely or partially controlled. None possess the level of artefact that this study does. It should come as no surprise that these procedures, when applied to these data, are not sufficient to totally eliminate the artefact. To emphasise resilience across research contexts and practicality of usage, no supervised learning approaches were used in this work.

In this study, we evaluated isolation forest [9], Knearest neighbour (KNN) distance [10], and 1-class support vector machine (SVM) [11] as three unsupervised machine learning techniques for artefact detection. For every half-second window, we established a set of 12 attributes that served as inputs for all unsupervised learning techniques. These 12 features were created by adding features that codify what is observably different by eye and using features already employed by current methods. Additionally, we contrasted the results with the current approaches. We discovered that none of the previous techniques could successfully remove heavy artefact from EDA data across all 6 subjects, but the unsupervised machine

learning algorithms using the features we defined could.

We go over the specifics of our datasets, identified features, and how we implemented the unsupervised learning methods in Methods. In the Results section, we present the EDA datasets both pre- and post-artifact, utilising every technique covered in the paper (including pre-existing techniques). Lastly, we discuss the consequences of our study and our ideas for further research in the section titled Discussion and Conclusion.

METHODS

A. Information

We used EDA data from six subjects—two of whom were female—for this investigation, obtained in accordance with a procedure that was authorised by the Human Research Committee at Massachusetts General Hospital (MGH). At MGH, all participants were having laparoscopic gynaecologic or urologic surgery. Using the Thought Technology Neurofeedback System [12], the EDA data were recorded from the first two digits of each subject's left hand at 256 Hz, beginning prior to the administration of anaesthesia and ending shortly after extubation. An example of raw data from a single individual is shown in Figure 1. The use of surgical cautery and movement at the start and finish, including placement, were the primary contributors of artefact. Every time cautery was turned on or off, the data showed a discernible deflection. Matlab 2020b was used to analyse all of the data.

B. Characteristics and Methods of Unsupervised Learning

Table 1 contains a list of the 12 qualities that were defined using literature guidance. To match the timing of individual artefacts, these features were estimated for each dataset for a 0.5 second window (128 samples). Three unsupervised learning techniques were then fed these feature vectors as inputs.

Using Euclidean distance and K of 50 in this example, KNN distance calculates the average distance between each feature vector and the K nearest feature vectors in the data set [10]. It is predicted that artifactual data will have a higher KNN distance than regular data [10]. While 1-class SVM is trained on data that is all labelled as a single class reflecting "normal" data, it is different from standard SVM. These might potentially include anomalies that are thought to be uncommon [11]. 90% of the data in this

instance were used to train the 1-class SVM, with the exception of the 10% with the largest KNN distance. Similar to random forests, isolation forests rank each feature vector as a leaf in a forest of decision trees by calculating the average length of the path. It is assumed that path lengths in artifactual data are shorter than in regular data [9]. The isolation scores in this instance were calculated as the median of ten forests, with each isolation forest having 100 decision trees.

TABLE I. FEATURES

	Feature Description
1	Standard deviation of signal
2	Difference between max and min of signal
3	Mean of first derivative
4	Median of first derivative
5	Standard deviation of first derivative
6	Min of first derivative
7	Max of first derivative
8	Mean of level 4 Haar wavelet coefficients
9	Median of level 4 Haar wavelet coefficients
10	Standard deviation of level 4 Haar wavelet coefficients
11	Min of level 4 Haar wavelet coefficients
12	Max of level 4 Haar wavelet coefficients

For every window of data, the three unsupervised learning techniques produced scores that indicated how anomalous that particular portion of the data was (the isolation forest scores, or IF scores, were made negative to match the directionality of the others). The process's final stage involved setting a threshold for each subject's scores in order to identify artefact. The method used to choose these thresholds was based on the realisation that the parts of the data that are classified as artefacts drop non-continuously, in discontinuous leaps, as the threshold is raised for each dataset. Since the inter-artifact interval distribution would get more skewed as the proportion artefact drops, this was taken advantage of by computing the skewness and kurtosis (3rd and 4th moments) of the distribution across thresholds.

We examined the criteria for local maxima in skewness and kurtosis (significant change in labelled artefact). The threshold determination process was optimised to verify no more than five criteria for each

unsupervised learning method per subject by using a binary search strategy within this collection of thresholds. Visual inspection was used to determine the ultimate threshold, which guaranteed artefact eradication.

The artefact was located and eliminated, and then linear interpolation was used to fill in the gaps and produce continuous data. The linearly interpolated mean of the data at that point was used to translate any "islands" of data that had moved uphill or lower as a result of artifactual deflection. In the end, we contrasted our approach with three other approaches that are currently in use: wavelet decomposition [6,7], variational mode decomposition [4,5], and straightforward hardcoding of heuristic rules based on thresholding the data derivative.

RESULTS

The outcomes of the three unsupervised techniques for each of the six participants are compiled in Table II. The maximum contiguous length of artefact and the proportion of artefact from 0 to 1 are provided for each subject and method. For each participant, the optimal approach is indicated in bold by the shortest contiguous length of artefact and the smallest fraction of artefact removed (removing the least amount of extra signal).

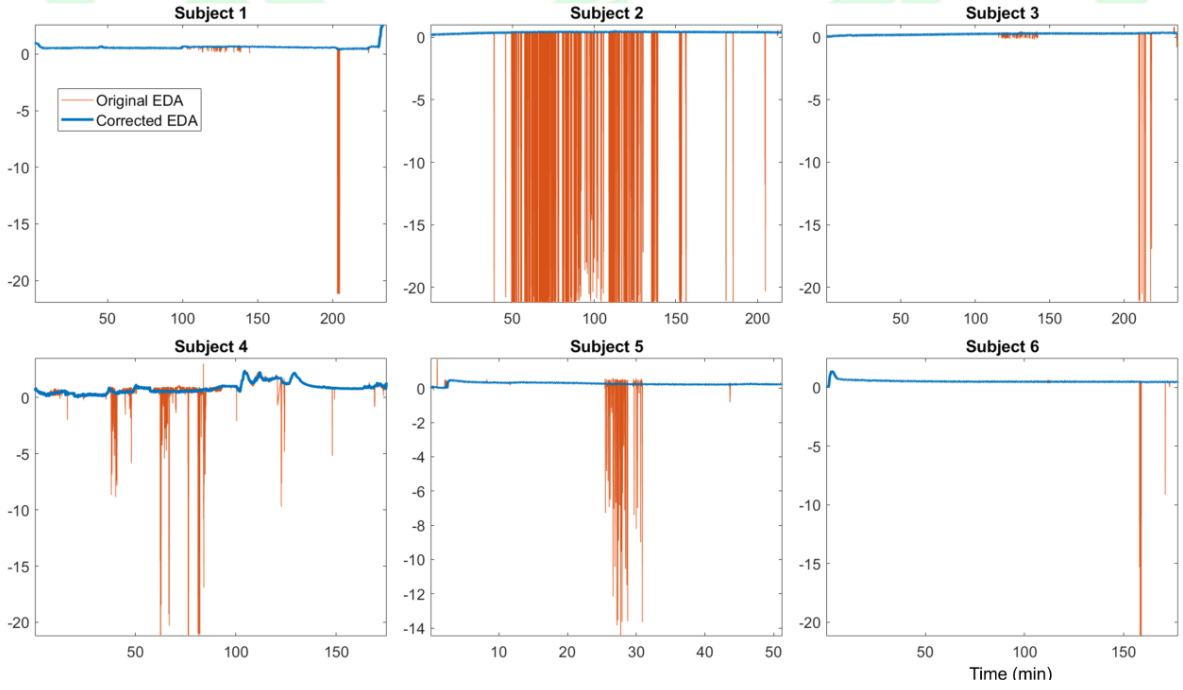

Figure 2. Uncorrected and corrected EDA for all 6 subjects.

For three of the six subjects, isolation forest proved to be the most effective approach; for one subject, each of the KNN distance and 1-class SVM techniques was equally effective. The longest contiguous artefact varied from 6 seconds to 106 seconds, while the quantities of artefact varied from less than 1% to slightly over 10% for every participant.

TABLE II. SUMMARY OF RESULTS

Subj	Proportion artifact Max contiguous length of artifact (sec)		
	Isolation Forest	*KNN Distance*	*1-class SVM*
1	0.0876 17.5039	0.0729 17.5039	**0.0321**[a] **17.5039**
2	**0.1030** **26.0039**	0.1169 26.5039	0.1314 26.5039
3	**0.0361** **28.5039**	0.0398 28.5039	0.0422 28.5039
4	**0.0191** **105.5659**	**0.0191** **105.5659**	**0.0191** **105.5659**
5	0.1000 14.5039	**0.0974** **14.5039**	0.1062 14.5039
6	**0.0062** **6.0039**	0.0225 6.0039	0.0149 13.5039

All six participants' EDA data, both uncorrected and final corrected, are displayed in Fig 2. Although the artifact's degree differed throughout participants, we were always able to eliminate it. An example of determining the ideal threshold for Subjects 2 and 4 using the kurtosis of the inter-artifact interval distribution is presented in Fig. 3. Based on a visual evaluation of the corrected EDA data, the highlighted values were chosen as the final thresholds after testing the local maxima of the kurtosis, as depicted in Fig 3.

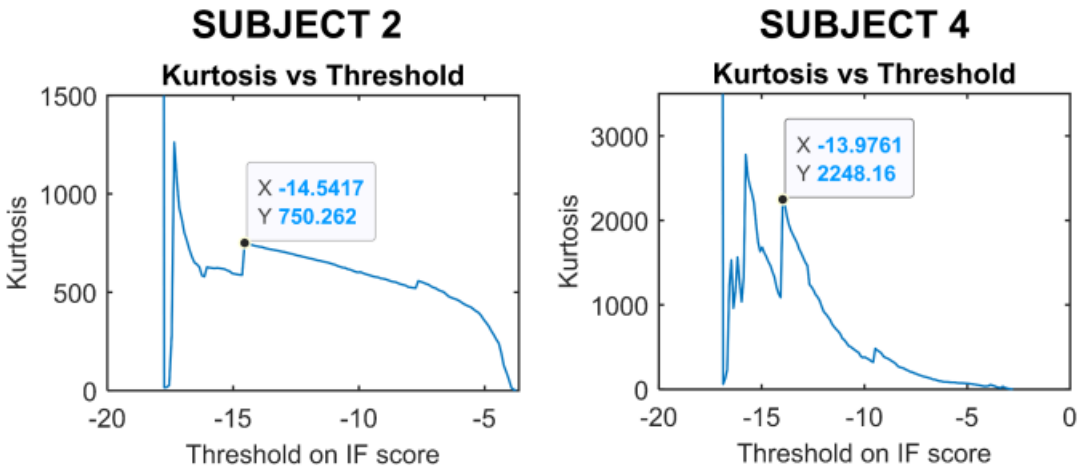

Figure 3. Use of kurtosis of inter-artifact interval distribution to select thresholds for Subjects 2 and 4. IF score refers to isolation forest score.

Lastly, for Subjects 2 and 4, Fig. 4 compares our approach with a number of other methods now in use. Only our method completely removed the artefact among the methods compared; hardcoding heuristic rules to threshold the derivative of the EDA signal or thresholding the EDA signal at 0 were both ineffective. Variational mode decomposition and wavelet decomposition were the only methods that showed some effectiveness.

DISCUSSION

In this work, we employed unsupervised machine learning techniques together with a collection of 12 features that we established in order to eliminate movement-related artefact and heavy cautery from EDA data that was obtained from 6 patients during surgery. Three unsupervised learning techniques—isolation forest, KNN distance, and 1-class SVM—were contrasted with three other approaches that had already been developed: wavelet decomposition, variational mode decomposition, and hardcoded heuristic rules. Only the unsupervised learning techniques were able to completely eliminate the artefact for each of the six subjects. We minimised the quantity of surplus EDA signal deleted together with artefact to determine which unsupervised learning strategy was optimum for each individual.

This approach is noteworthy since it eliminated heavy artefact while eliminating the need for human labelling of a training data set. Furthermore, our approach made it possible to preserve as

much of the genuine EDA signal as possible, even when it was split up throughout different artefact portions. The actual percentage of data recognised as artefact, even in circumstances of visually intense artefact, was probably 10% or less; any thresholding-based approach would have probably eliminated a far larger percentage of the data, including legitimate EDA signal. Additionally, the majority of currently used techniques use decomposition algorithms that have the ability to alter any part of the signal, including those that are obviously artifact-free.

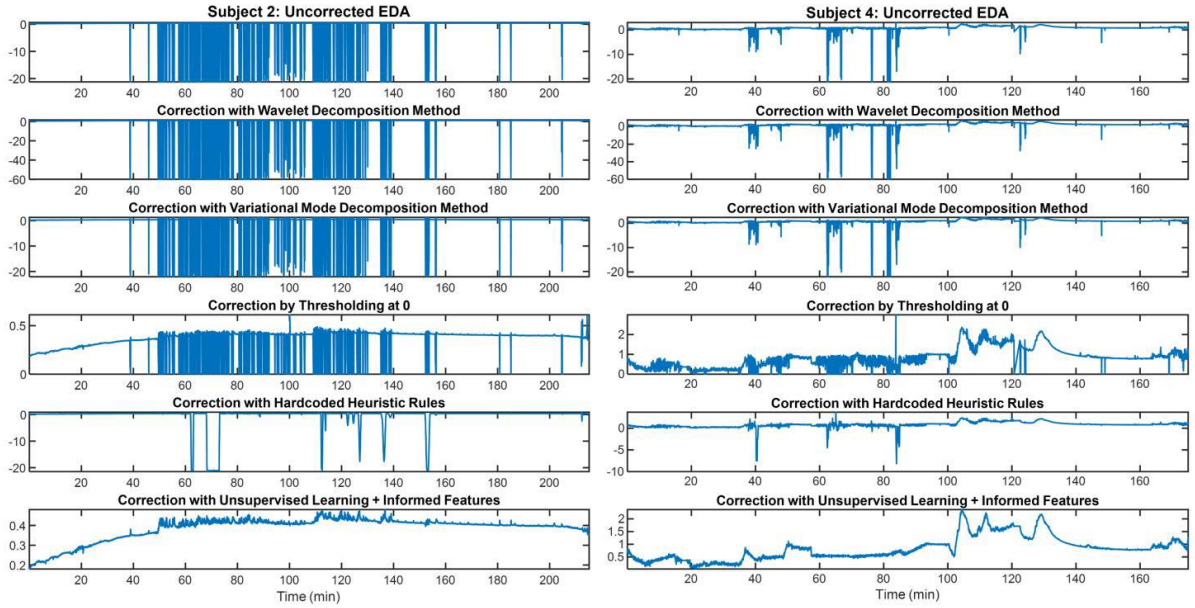

Figure 4. Comparison between different methods for Subjects 2 and 4.

In contrast, non-artifact areas of the raw data remain unaltered by our method. The longest continuous artefact was less than 30 seconds for 5 out of the 6 patients and less than 20 seconds for 3 out of 6 subjects, indicating that the majority of this artefact was eliminated in extremely brief parts.

The tonic and phasic components, which include complimentary information and function at separate timeframes, are the two components that are commonly used to analyse EDA [3]. Short stretches of artefact allow for easy interpolation of the tonic component, which drifts progressively over tens of seconds to minutes [3]. Short data lengths (less than 30 seconds) for phasic EDA are unlikely to contain more than a few pulses [3]. Moreover, even in cases when a few pulses are absent for brief periods of time,

dynamic approaches can calculate the mean and standard deviation of pulse rate over time and adjust the estimate of uncertainty accordingly [13].

Lastly, our approach only utilised 12 features per window, and a large number of these features were duplicated in other approaches. But with each dataset, our approach enabled AI to "learn" the distinctions between artefact and signal. The physiology of EDA data was taken into consideration when developing these 12 aspects. Our approach is readily extendable to other types of "easily visible" artefact in other physiological data modalities, such ECG and EEG. Awareness of the physiology and types of artefact in the data can help define custom features.

Financial support and sponsorship: Nil

Conflict of Interest: None

REFERENCES

[1] G. Biagetti, P. Crippa, L. Falaschetti, G. Tanoni, C. Turchetti, "A comparative study of machine learning algorithms for physiological signal classification," *Procedia Computer Science*, vol. 126, pp. 1977- 1984, 2018.

[2] M. Goldstein, S. Uchida, "A Comparative Evaluation of Unsupervised Anomaly Detection Algorithms for Multivariate Data," *PLoS ONE*, vol. 11, no. 4, pp. e0152173, Apr 2016.

[3] W. Boucsein, *Electrodermal Activity*. New York, NY: Springer, 2012.

[4] C. Qi, R.T. Faghih, "Detection of Autonomic Sympathetic Arousal from Electrodermal Activity," PowerPoint presentation (unpublished).

[5] K. Dragomiretskiy, D. Zosso, "Variational Mode Decomposition," *IEEE Trans. Sig. Proc.*, vol. 62, no. 3, pp. 531-544, Feb. 2014.

[6] W. Chen, N. Jacques, S. Taylor, A. Sano, S. Fedor, R. W. Picard, "Wavelet-Based Motion Artifact Removal for Electrodermal Activity," in *Conf. Proc. IEEE Eng. Med. Biol. Soc.*, pp. 6223-6226, Aug 2015.

[7] S. Taylor, N. Jacques, W. Chen, S. Fedor, A. Sano, R. Picard, "Automatic Identification of Artifacts in Electrodermal Activity Data," in *Conf. Proc. IEEE Eng. Med. Biol. Soc.*, pp. 1934-1937, Aug 2015.

[8] Y. Zhang, "Unsupervised Motion Artifact Detection in Wrist-Measured Electrodermal Activity Data," M.S. thesis, Dept. Electric. Eng., Univ. of Toledo, Toledo, Ohio, 2017.

[9] F. T. Liu, K. M. Ting, Z-H. Zhou, "Isolation Forest," in *Proc. 8th IEEE Int. Conf. Data Mining*, pp. 413-422, 2008.

[10] L-Y. Hu, M-W. Huang, S-W. Ke, C-F. Tsai, "The distance function effect on k-nearest neighbor classification for medical datasets," *SpringerPlus*, vol. 5, no. 1304, Aug 2016.

[11] L. M. Manevitz, M. Yousef, "One-Class SVMs for Document Classification," *Journal of Machine Learning Research*, vol. 2, pp. 139- 154, 2001.

[12] "Neurofeedback Expert System", Thought Technology Ltd, https://thoughttechnology.com/neurofeedback-expert-system/, accessed 1/6/21.

[13] R. Barbieri, E. C. Matten, A. A. Alabi, E. N. Brown, "A point-process model of human heartbeat intervals: new definitions of heart rate and heart rate variability," *Am. J. Physiol. Heart Circ. Physiol.*, vol. 288, no. 1, pp. H424–435, Jan 2005.